Electrophoretic transport and molecular control at nanoscale

Author: Lucas Santiago Palacios Ruiz.

Facultat de Física, Universitat de Barcelona, Diagonal 645, 08028 Barcelona, Spain.[*]

Abstract: In this work we look for an analytical result for electrophoresis mobilities for a single rod under an applied constant electric field. We obtained that $\mu = \mu(\kappa a, \kappa L, a/L)$ and consequently, we study asymptotic regimes. Finally, we tried to study a similar problem with computer simulations using Verlet algorithm but it was impossible to achieve a correct solution.

I. INTRODUCTION

Nowadays, biological systems are increasing in importance due its direct function in industrial applications and health care. Since its significative importance, one can try to study the physics behind these systems. Although they can be large and variable, there are always structures that recure in it as biopolymers. Biopolymers are a big family of polymers that have a significative biological function. As an example of them, we can focus on proteins but it would be also possible to focus on DNA or RNA. Proteins are one of the key pieces in biological systems and are rolled in almost every process in them. Structullary, proteins are made by organic molecules called amino acids that are connected making a chain or in our nomenclature, a biopolymer. Although this simple definition can let us to think that proteins can be quite linear, in fact proteins also need to be folded in a correct way to do a function and therefore, many times are seen as globular molecules which interact with the surrounding medium by electrical forces. Even though this new conformation is very common, it is also true that one can always unfold them with some chemical products and thus working with them with a quite linear form. Apart from this constructions, we have also to consider that proteins can be the basic elements to build bigger structures. As a result of it, one can always imagine that it is possible to build a new biopolymer considering now proteins as amino acids in the previous explanation. These new structures are also seen very frequently in nature as we can see with microtubules and actin, which are present in every eukaryotic cell to hold their structure and to be the pathway to transport different elements inside the cells. The study of these structures are not only important for medical advances but also they can be effective for other fields such as nanoengineering due to the analogy that we can make with new nano polymers that we are being able to build as carbon nanotubes which are carbon polymers with great implications in a near future.

Related to biopolymers, there is a standard mechanism that has been used since many years ago to distinguish proteins called electrophoresis, which is one of the simplest ways to discriminate proteins. This technique consists in applying an electric field to a fluid that contains proteins to distinguish them by their mobility. The reason of this procedure is based on the fact that, as we pointed before, proteins in a solution have a charged interface between their surface and the surrounding fluid. As a result of it, we can see a movement of the protein that is opposed to the present in the fluid but with a null neat force as we can see in the work of M.G.L. van den Heuvel et al[1] with microtubules. This motion is ususally referred to as phoretic since the protein is being carried inside a fluid.
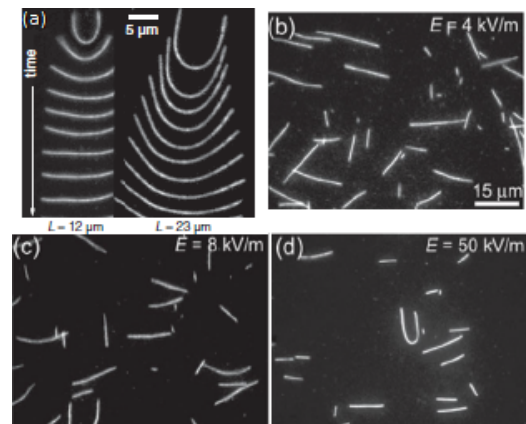
FIG. 1: Experiment done with microtubules by M.G.L. van den Heuvel et al[1]. (a) Relaxation of 2 different microtubules after switching of the electric field. Snapshots are shown with 0.1 s time interval. Microtubules measured at different electric fields of (b) E=4 kV/m, (c) 8 kV/m, and (d) 50 kV/m. In all images the electric field points upwards (microtubules move downward).

In this work we analyse how a biopolymer responds in a fluid medium under the action of an applied constant electric field. As we will see, this response will depend on the magnitude of the electrical field, the charge of the protein and other geometrical properties. Because of its complexity, firstly we do our analysis considering the extreme condition that our protein can be characterized as a finite solid rod. After this analysis, we tried to simulate this problem under more realistic conditions so we can imagine the protein as a flexible chain that reminds us a more similar condition to microtubules inside a real cell.

———————

[*]Electronic address: `lpalacru7@alumnes.ub.edu`

II. PHYSICAL THEORY

As we have explained before, we consider a solid rod of radius a and length 2L inside a fluid. To solve this problem we can start from Navier-Stokes equations but before going on, we might have to have some considerations about boundary conditions. Uses of electrophoresis always take place in medium with low Reynolds and always take long time to achieve because of the slow movement of the fluid. Due to this fact, we know that we are going to work with an incompressible flow and given that our velocity field is going to be small, we can consider the Stokes solution for an incompressible fluid as follows in equation (1):

$$
\begin{aligned}
-\nabla p + \eta \Delta \mathbf{v} + \mathbf{f_{ext}} &= \mathbf{0} \\
\nabla \cdot \mathbf{v} &= \mathbf{0}
\end{aligned} \tag{1}
$$

By doing a Fourier transform to (1) and solving for $\mathbf{v}$ we get:

$$
\mathbf{v}(\mathbf{q}) = \frac{1}{\eta q^2}\left(\mathbb{1} - \frac{\mathbf{qq}}{q^2}\right)\cdot\mathbf{f_{ext}} \tag{2}
$$

Now if we make the inverse Fourier transform of Eq. (2) we will get the velocity field in real space[2]. Considering that the external force is a constant electrical field $\mathbf{E}$ which interacts with a charge distribution $\Psi(\mathbf{r})$ then Eq. (2) can be written as:

$$
\mathbf{v}(\mathbf{r}) = \int \frac{dr'}{8\pi\eta|r-r'|}\left[\mathbb{1} + \frac{(\mathbf{r}-\mathbf{r}')(\mathbf{r}-\mathbf{r}')}{|r-r'|^2}\right]\Psi(\mathbf{r})\cdot\mathbf{E} \tag{3}
$$

Trying to solve (3) can be very complex and so we try to get around by taking the velocity at some point $\mathbf{r_1} = z_0\widehat{\mathbf{e_z}}$ over the surface of the rod and integrating this velocity for all points over the cylinder and in all the space except inside the rod. By doing this, we will know the velocity that drags our rod and hence the mobility of the rod. Since we have a rod, we get cylindrical coordinates to resolve this problem. If we integrate over the angle direction and over all points of the rod we get a large expression that can be expressed in terms of perpendicular and parallel components of $\mathbf{E}$ as it is shown in Eq. (4).

$$
\begin{aligned}
v_{||} &= \int_0^\infty d\rho\frac{\rho+a}{4\eta}\int_{-L}^L dz\Psi(r)\frac{(\rho+a)^2+2(z-z_0)^2}{\sqrt{(\rho+a)^2+(z-z_0)^2}}E_{||} \\
v_\perp &= \int_0^\infty d\rho\frac{\rho+a}{8\eta}\int_{-L}^L dz\Psi(r)\frac{3(\rho+a)^2+2(z-z_0)^2}{\sqrt{(\rho+a)^2+(z-z_0)^2}}E_\perp
\end{aligned} \tag{4}
$$

From Eq. (4) not only it is easy to obtain the parallel and perpendicular electrophoretic mobilities $\mu_{||(\perp)} = v_{||(\perp)}/(2\pi E_{||(\perp)})$ but also shows clearly that mobilities depend on our charge distribution but are independent of the magnitude of the electric field in the linear regime. As we are working with biopolymers that have a surface charge density, we can study the easiest case in which this charge density is uniform and therefore $\Psi(\mathbf{r})$ will depend on this density. Due to the fact that the surrounding medium has dissolved salts in it we need to add a contribution from the fluid. In a first approximation, we can consider that the charge density distribution caused by all salts will be in equilibrium with the density of the rod creating a diffuse layer that balances the charge of the rod and therefore, ensures global electroneutrality. To reach an expression for this density we can resolve Poisson equation in cylindrical coordinates. As we are in equilibrium, we can include this condition using Boltzmann statistics to calculate the charge density distribution. By combining both equations, it is possible to get the so-called Poisson-Boltzmann equation. For a small charge of the rod, the solution of this equation can be written explicitly in terms of a modified Bessel function of the second kind for an infinite cylinder [3]. In our work, considering infinite length is a good approximation as a biopolymer can measure not only μm in length but also nm in diameter. These sizes let us to say that $L/a \to \infty$ so we can consider that the effects over the extremes are negligible. As a result of these considerations we have that $\Psi(\mathbf{r})$ can be described only on terms of the cylindrical radius as seen in equation (5).

$$
\begin{aligned}
\Psi(\rho) &= \Psi_r(\rho) + \Psi_{dl}(\rho) = \\
&= \frac{Q}{4\pi La}\delta(\rho-a) - \frac{Q\kappa}{4\pi LaK_1(\kappa a)}K_0(\kappa\rho)
\end{aligned} \tag{5}
$$

Notice that with (5) we have introduce the inverse of Debye screening length κ. Using (5) in (4) retrieves the mobilities that we are looking for but as (5) implies a modified Bessel function of the second kind, the intregal is not easy and therefore, the detailed derivation of the electrophoretic mobilities is described in the Appendix. The main results that come out of the general derivation correspond to the parallel and perpendicular mobilities, which have a contribution due to the rod charge, μ_r, and a contribution from the diffuse ions around the rod, μ_{dl}. The general expression indicates that the electrophoretic mobility sdepends on three dimensionless parameters $\mu = \mu(\kappa a, \kappa L, a/L)$. This dependence can be expressed as,

$$
\begin{aligned}
\mu_{||,r} &= \frac{3Q}{4\pi^2\eta}\left[\frac{a}{L} - \sqrt{\left(\frac{a}{L}\right)^2+1} + \tfrac{1}{3}ln\left(\frac{\sqrt{\left(\frac{a}{L}\right)^2+1}+1}{\sqrt{\left(\frac{a}{L}\right)^2+1}-1}\right)\right] \\
\mu_{\perp,r} &= \frac{Q}{8\pi^2\eta}\left[\frac{a}{L} - \sqrt{\left(\frac{a}{L}\right)^2+1} + ln\left(\frac{\sqrt{\left(\frac{a}{L}\right)^2+1}+1}{\sqrt{\left(\frac{a}{L}\right)^2+1}-1}\right)\right]
\end{aligned} \tag{6}
$$

$$\mu_{||,dl} = -\frac{3Q}{16\pi^2\eta}\left\{\frac{\pi}{2\kappa L}\left[\frac{1}{\kappa a}\left(1-\frac{2}{\pi}\frac{1}{\kappa L}\right)-\frac{K_2(\kappa L)}{\pi}\frac{a}{L}+K_1(\kappa a)L_0(\kappa a)+K_0(\kappa a)L_1(\kappa a)-3(K_1(\kappa a)L_2(\kappa a)+K_2(\kappa a)L_1(\kappa a))\right]\right.$$

$$-2\left[\frac{1}{\kappa a}+\frac{1}{3}K_1(\kappa a)\left(\ln\left(\frac{\sqrt{\left(\frac{a}{L}\right)^2+4}+2}{\sqrt{\left(\frac{a}{L}\right)^2+4}-2}\right)-\frac{4}{\sqrt{\left(\frac{a}{L}\right)^2+4}}-3\right)+\frac{2\pi\kappa a}{3\sqrt{\left(\frac{a}{L}\right)^2+4}}\left(\frac{1}{\kappa a}-K_0(\kappa a)L_{-1}(\kappa a)-L_0(\kappa a)K_{-1}(\kappa a)\right)\right]$$

$$\left.+\frac{K_3(\kappa a)}{4}\left(\frac{a}{L}\right)^2-\frac{L}{2a}(2\kappa L)^{-\frac{1}{2}}S_{\frac{1}{2},\frac{3}{2}}(2\kappa L)\right\}$$

$$\mu_{\perp,dl} = -\frac{Q}{32\pi^2\eta}\left\{\frac{\pi}{2\kappa L}\left[\frac{1}{\kappa a}\left(1-\frac{2}{\pi}\frac{1}{\kappa L}\right)-\frac{K_2(\kappa L)}{\pi}\frac{a}{L}+K_1(\kappa a)L_0(\kappa a)+K_0(\kappa a)L_1(\kappa a)-3(K_1(\kappa a)L_2(\kappa a)+K_2(\kappa a)L_1(\kappa a))\right]\right.$$

$$-2\left[\frac{1}{\kappa a}+K_1(\kappa a)\left(\ln\left(\frac{\sqrt{\left(\frac{a}{L}\right)^2+4}+2}{\sqrt{\left(\frac{a}{L}\right)^2+4}-2}\right)-\frac{4}{\sqrt{\left(\frac{a}{L}\right)^2+4}}-1\right)+\frac{2\pi\kappa a}{\sqrt{\left(\frac{a}{L}\right)^2+4}}\left(\frac{1}{\kappa a}-K_0(\kappa a)L_{-1}(\kappa a)-L_0(\kappa a)K_{-1}(\kappa a)\right)\right]$$

$$\left.+\frac{K_3(\kappa a)}{4}\left(\frac{a}{L}\right)^2-\frac{L}{2a}(2\kappa L)^{-\frac{1}{2}}S_{\frac{1}{2},\frac{3}{2}}(2\kappa L)\right\}$$

$$(7)$$
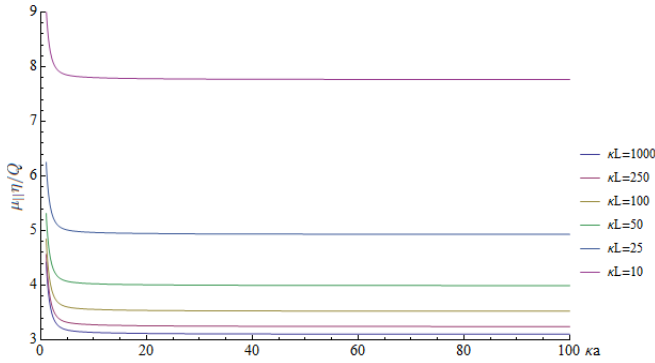
FIG. 2: Some values obtained for $\mu_{||}$ with a/L=0.001
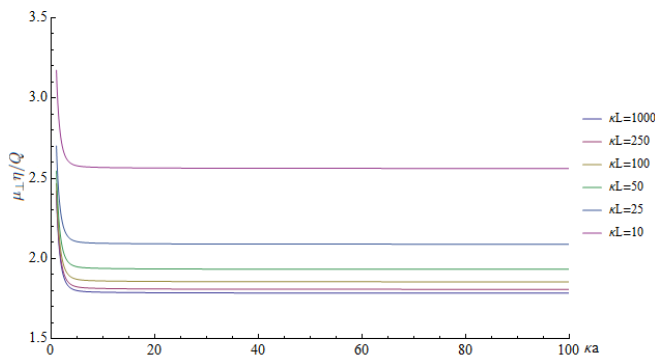
FIG. 3: Some values obtained for $\mu_{\perp}$ with a/L=0.001

For a charged rod, L and a can be regarded as constant, while kappa and **E** can be regarded as natural tuning parameters. Accordingly, we plot some regions of both expressions to try to visualize them in figures 2 and 3. Now that we have a better idea, we can think about the physical meaning of the behavior of the electrophoretic mobility as a function of the rod asymmetry and its response to changes in salt concentration. Both products can be seen as double layer structures along the axis of our cylinder or perpendicular to it. The dependence of μ on three dimensionless parameters allows us to identify three different regimes that characterize how the rod will react to an applied electric field:

- $\kappa L \gg 1, \kappa a \gg 1$ or thin double layer.

- $\kappa L \gg 1, \kappa a \ll 1$ or intermediate double layer.

- $\kappa L \ll 1, \kappa a \ll 1$ or wide double layer.

Nonetheless, we expect that κL will be a more relevant parameter than κa as we have a very long cylinder. These regimes suggest that it is worth identifying the asymptotic limiting regimes of the electrophoretic mobility asymmetry for very wide and very thin double layers. In our work we consider these limits only to see how the relation between components of the mobility is. If we take any of the two first limits we obtain:

$$\frac{\mu_{||}}{\mu_{\perp}}=\frac{\mu_{||_r}+\mu_{||_{dl}}}{\mu_{\perp_r}+\mu_{\perp_{dl}}}=2 \qquad (8)$$

This result reminds us the one found by resolving the ratio of perpendicular and tangential mobilities for a sedimenting uncharged rod[5] which is in line with Eq. (8).

On the other hand, the third limit verifies:

$$\frac{\mu_{||}}{\mu_{\perp}} = \frac{\mu_{||_r} + \mu_{||_{dl}}}{\mu_{\perp_r} + \mu_{\perp_{dl}}} = 6 \qquad (9)$$

which is not recorded in any known theory and therefore, we have obtained a new class of mobilities. After these results, we can see that our assumption that κL would be more important than κa is confirmed as we can see that κL prevails over κa due to the fact that if $\kappa L \gg 1$ we see that there is a continuity with no consideration of κa. In contrast to κa, variations over κL show us that there is a great sensitivity over this parameter.

Finally, it is also interesting to see how these limits approach to their solution. Although we wanted to show an approximation for every limit we figure out that in the first case there was not a correct development of Struve function at infinity and therefore, we were not able to show this limit. The result for the rest is shown in (10) for $\kappa L \gg 1, \kappa a \ll 1$ and in (11) for $\kappa L \ll 1, \kappa a \ll 1$.

$$\frac{\mu_{||}}{\mu_{\perp}} = 6 \left[1 - \frac{2}{3} \frac{2\left(ln\left(\frac{a}{L}\right)+1\right) + \pi \kappa a \left(1 - \frac{2\left(ln\left(\frac{a}{L}\right)+1\right)}{2ln\left(\frac{a}{L}\right)-1}\right)}{2ln\left(\frac{a}{L}\right)-1} \right] \qquad (10)$$

$$\frac{\mu_{||}}{\mu_{\perp}} = 6 \left[1 - \frac{4}{3} ln\left(\frac{a}{L}\right) \kappa L \right] \qquad (11)$$
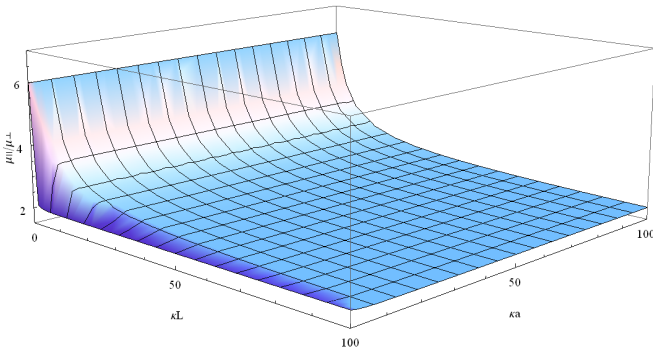
FIG. 4: Some values obtained for $\mu_{||}/\mu_{\perp}$ with a/L=0.001

III. COMPUTER SIMULATIONS

Once we obtained our analytical result, we tried to simulate this problem with a flexible rod with only performing a perpendicular constant force $\mathbf{F}_{\perp}$. For this purpose we have simulated this problem with a flexible chain of n elements under Verlet algorithm. Unlike other works where the simulation has been done with

an hydrodynamic velocity given by the Oseen tensor[6] here we present an hydrodynamic velocity given by the solution of the electrophoresis [7]. The interest of this change is because of the nature of the problem. With a charged particle, it is necessary to include the fact that our particle has a double layer around it which is not included with only the Oseen tensor.

With this idea in mind, we have simulated a flexible chain of 30 elements with different forces under two regimes of Debye length:

- High value ($\kappa/L = 1000$) or intermediate double layer.

- Low value ($\kappa/L = 0,001$) or wide double layer.

After doing the simulations we have studied the shape of the chains and we have looked for the friction coefficient once the chain has arrived to a steady state. Friction coefficient has been obtained from the average velocity of the chain printed by our code and following expression (12).

$$\gamma = \frac{F_{\perp}}{\langle v \rangle} \qquad (12)$$

To reach these goals we were going to present two types of graphics. On one hand we wanted to present a characteristic transverse distortion A/L defined as the distance between the uppermost and the lowermost point of the chain along the direction of $\mathbf{F}_{\perp}$ normalized to the length of the chain as a function of a dimensionless force defined by:

$$B = \frac{L^3 F_{\perp}}{k} \qquad (13)$$

where k is the stiffness of the chain.

On the other hand, we also wanted to present the results of the friction coefficients but normalised to its value in the stiff limit (γ_0) and as a function of B. Although our idea was clear, we were not able to study these parameters as our system was not evolving appropriately. We figured out this conclusion after seeing results as the ones presented in figures (5) and (6).

IV. CONCLUSIONS

Eq. (6) and (7) show that it is possible to distinguish charged particles with a uniform charged rod shape with L/a$\rightarrow \infty$ only by its mobility due to the fact that $\mu = \mu(\kappa a, \kappa L, a/L)$. Furthermore, these expressions also show that κL prevails over κa only if $\kappa L \gg 1$. In this limit we see that our solution approaches the same solution as in the sedimenting uncharged rod but we cannot confirm if this approach is due to a deep physical behaviour since we have not compared the first terms of
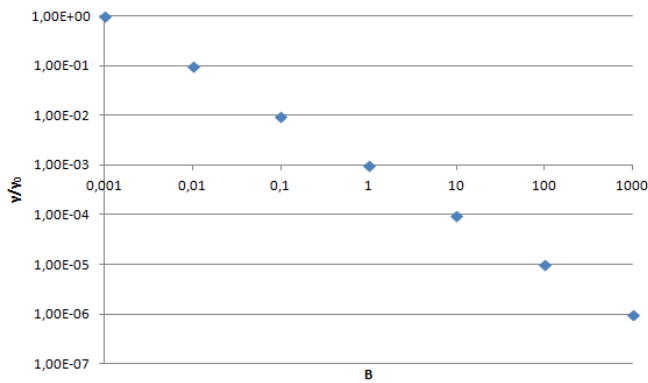
FIG. 5: Friction coefficient for large values of kappa ($\kappa/L =$ 1000) as a function of B. As it can be seen, this solution shows us that $\gamma = \langle v \rangle / F_{\perp}$ which cannot be because of Eq. (12).
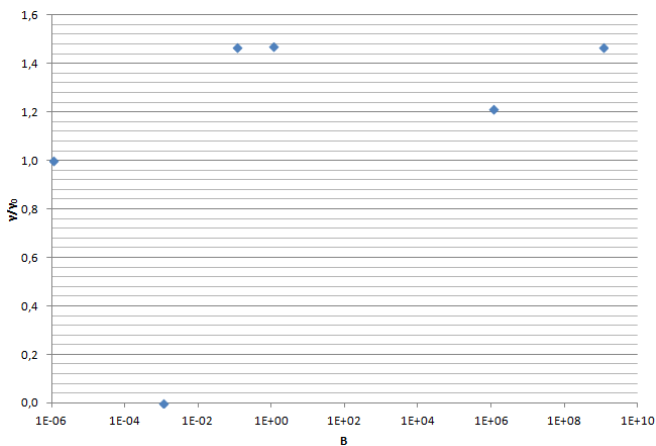
FIG. 6: Friction coefficient for large values of kappa ($\kappa/L =$ 1000) as a function of B. This figure differs from figure (5) in the fact that other parameters were changed.

the development of both theories. In contrast, we can see that when $\kappa L \ll 1$ this approach is not equal and both theories differ.

As a way to advance more in our research, we also performed some simulations using Verlet algorithm. Although this is a feasible way to study these movements in a deeper way, we were not able to evolve the system accordly as we could see with the studies performed over the friction coefficient. However, we think that this is a needed way to advance in our studies as it seems very difficult to continue our research with an analytical theory and therefore, it will be more studied in subsequent works in the next months.

Acknowledgments

[1] M.G.L. van den Heuvel *et al*, *Single-Molecule Observation of Anomalous Electrohydrodynamic Orientation of Microtubules*, Phys. Rev. Lett. 101, 118301 (2008).
[2] Masao Doi, *Introduction to polymer physics*, 1rd. ed. (Oxford university Press Inc., New York, United States, 1995).
[3] Jean-Louis Barrat and Jean-Pierre Hansen, *Basic concepts for simple and complex liquids*, 1rd. ed. (The press syndicate of the university of Cambridge, Cambridge, UK, 2003).
[4] G. N. Watson, *A treatise on the theory of Bessel functions*, 1rd. ed. (The press syndicate of the university of Cambridge, Cambridge, UK, 1922).
[5] M. Doi and S. F. Edwards, *The Theory of Polymer Dynamics*, 1rd. ed. (Oxford university Press Inc., New York, United States, 1994).
[6] M. Cosentino Lagomarsino *et al*, *Hydrodynamic Induced Deformation and Orientation of a Microscopic Elastic Filament*, Phys. Rev. Lett. 94, 148104 (2005).
[7] D. Long *et al*, *A note on the screening of hydrodynamic interactions, in electrophoresis, and in porous media*, Eur. Phys. J. E 4, 29-32 (2001).
[8] I.S. Gradshteyn and I.M. Ryzhik, *Table of Integrals, Series, and Products*, 7th. ed. (Elsevier Academic Press publications, USA, 2007)

APPENDIX A: DETAILS ON THE ANALYTICAL SOLUTION

If we integrate mobilities using Eq. (4) over all points $\mathbf{r_1}$ of our rod and over all the lenght of the rod we obtain:

$$
\begin{aligned}
\mu_{||} &= \int_0^\infty d\rho \frac{3(\rho+a)}{4\pi\eta}\Psi(\rho)\left[(\rho+a)-\sqrt{(\rho+a)^2+4L^2}+\frac{2L}{3}ln\left[\frac{2L+\sqrt{(\rho+a)^2+4L^2}}{-2L+\sqrt{(\rho+a)^2+4L^2}}\right]\right] \\
\mu_{\perp} &= \int_0^\infty d\rho \frac{\rho+a}{8\pi\eta}\Psi(\rho)\left[(\rho+a)-\sqrt{(\rho+a)^2+4L^2}+2Lln\left[\frac{2L+\sqrt{(\rho+a)^2+4L^2}}{-2L+\sqrt{(\rho+a)^2+4L^2}}\right]\right]
\end{aligned}
$$
(A1)

In this appendix we will focus on the solution for $\Psi(\rho) = K_0(\kappa\rho)$ as the delta term is easy to resolve. For this purpose, Eq. (A1) can be divided in three sections, one for every addend with independence of its prefactor.

Using some solutions presented in [8] and some properties of Bessel equations, one can archieve for the first addend a solution in terms of basically, modified Bessel functions of second kind and Struve functions (L_ν):

$$
\int_0^\infty d\rho(\rho+a)^2 K_0(\kappa\rho) = \frac{\pi}{2}\left[\frac{1}{\kappa^3}+\frac{a}{\kappa^2}(-3K_2(\kappa a)L_1(\kappa a)-3K_1(\kappa a)L_2(\kappa a)+K_1(\kappa a)L_0(\kappa a)+K_0(\kappa a)L_1(\kappa a))\right] \text{(A2)}
$$

Solution of the second addend is more difficult due to the fact that in this occasion, one can only find an integral without a simple solution that can be expressed in terms of $x = \frac{\rho+a}{a}$. Furthermore, with this solution we need to

introduce a new function called Lommel function ($S_{\frac{1}{2},\frac{3}{2}}$) which is derived from the Bessel theory[4].

$$
-\int_0^\infty d\rho(\rho+a)\sqrt{(\rho+a)^2+4L^2}K_0(\kappa\rho) = -\left[(2L)^3(2\kappa L)^{\frac{3}{2}}S_{\frac{1}{2},\frac{3}{2}}(2\kappa L)-2La^2\int_0^1 dxx\sqrt{\left(\frac{xa}{2L}\right)^2+1}K_0(\kappa ax)\right] \text{(A3)}
$$

This integral cannot be found in [8] nor Mathematica can resolve it but as long this integral is bounded and finite, we can consider the limit a/L$\to$ 0 and therefore we can

do a Taylor expansion of a/L. If we take the second order now it is possible to solve and we can say that:

$$
\int_0^1 dxx\sqrt{\left(\frac{xa}{2L}\right)^2+1}K_0(\kappa ax) \approx \frac{1}{(\kappa a)^2}-\frac{K_1(\kappa a)}{\kappa a}+\left(\frac{a}{2L}\right)^2\left(\frac{2}{(\kappa a)^4}+\frac{K_2(\kappa a)}{(\kappa a)^2}-\frac{K_3(\kappa a)}{2\kappa a}\right)
$$
(A4)

Finally, the third addend is the hardest one to integrate. As the previous integral, it cannot be found in [8] nor

Mathematica can resolve it. Using some complex vari-

able changes, one can find that there is always a new expression that also cannot be solved easily even if one try to solve these expressions using complex integrals or Taylor series. The best way to integrate it was found by

doing a change variable $\xi = \frac{\rho+a}{2L}$ and then doing a Taylor expansion in powers of series of ξ over $\xi\frac{\sqrt{\xi^2+1}+1}{\sqrt{\xi^2+1}-1}$ around $\frac{a}{2L}$. With these changes it is possible to get:

$$\int_0^\infty d\rho(\rho+a)K_0(\kappa\rho)\frac{2L}{3}ln\left[\frac{2L+\sqrt{(\rho+a)^2+4L^2}}{-2L+\sqrt{(\rho+a)^2+4L^2}}\right]=$$

$$=\frac{2aL^2}{3}\left[\frac{K_1(\kappa a)}{L\kappa}\left(ln\left(\frac{\sqrt{\left(\frac{a}{L}\right)^2+4}+2}{\sqrt{\left(\frac{a}{L}\right)^2+4}-2}\right)-\frac{4}{\sqrt{\left(\frac{a}{L}\right)^2+4}}\right)+\frac{2\pi a}{L\sqrt{\left(\frac{a}{L}\right)^2+4}}\left(\frac{1}{a\kappa}-K_0(a\kappa)L_{-1}(a\kappa)-K_{-1}(a\kappa)L_0(a\kappa)\right)\right]$$

(A5)

If we now add constant prefactors and resolve Eq. (A1) for the delta term, it is possible to obtain the result shown

in Eq. (6) for the component of constant charge in rod and Eq. (7) for the diffuse layer, respectively.